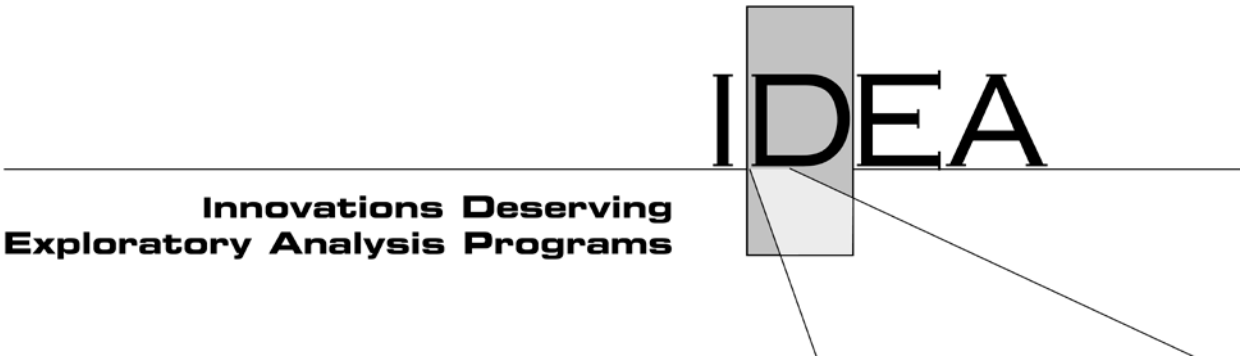

NCHRP IDEA Program

Laser Spectroscopy for Rapid Profiling of Steel Bridge Coating, Corrosion, and Heavy Metals

Final Report for
NCHRP IDEA Project 164

Prepared by:
Warren H Chesner, Chesner Engineering P.C.
Nancy J. McMillan, New Mexico State University

May 2015

TRB TRANSPORTATION RESEARCH BOARD
The National Academies of
SCIENCES · ENGINEERING · MEDICINE

Innovations Deserving Exploratory Analysis (IDEA) Programs Managed by the Transportation Research Board

This IDEA project was funded by the NCHRP IDEA Program.

The TRB currently manages the following three IDEA programs:

- The NCHRP IDEA Program, which focuses on advances in the design, construction, and maintenance of highway systems, is funded by American Association of State Highway and Transportation Officials (AASHTO) as part of the National Cooperative Highway Research Program (NCHRP).
- The Safety IDEA Program currently focuses on innovative approaches for improving railroad safety or performance. The program is currently funded by the Federal Railroad Administration (FRA). The program was previously jointly funded by the Federal Motor Carrier Safety Administration (FMCSA) and the FRA.
- The Transit IDEA Program, which supports development and testing of innovative concepts and methods for advancing transit practice, is funded by the Federal Transit Administration (FTA) as part of the Transit Cooperative Research Program (TCRP).

Management of the three IDEA programs is coordinated to promote the development and testing of innovative concepts, methods, and technologies.

For information on the IDEA programs, check the IDEA website (www.trb.org/idea). For questions, contact the IDEA programs office by telephone at (202) 334-3310.

IDEA Programs
Transportation Research Board
500 Fifth Street, NW
Washington, DC 20001

IDEA Program

Final Report

NCHRP 164

Laser Spectroscopy for Rapid Profiling of Steel Bridge Coating, Corrosion, and Heavy Metals

Prepared for the IDEA Program
Transportation Research Board
The National Academies

Warren H. Chesner
Chesner Engineering, P.C.
and
Nancy J. McMillan
New Mexico State University

May 11, 2015

ACKNOWLEDGMENTS

This work was funded by the Transportation Research Board of the National Academies under the TRB-IDEA Program (NCHRP-164). Special thanks is extended by the Research Team to the TRB Project Director, Inam Jawed, and the Advisory Panel: Georgene Geary, Georgia Department of Transportation; Josh Antelman, U.S. Naval Facilities Engineering Command; Beran Black, New Hampshire Department of Transportation; Winson King, Pennsylvania Department of Transportation; Peter Jansson, Michigan Department of Transportation; and Kieche Meleson, U.S. Naval Facilities Engineering Command.

The invaluable technical assistance of the firm of Corrosion Control Consultants & Labs, Inc. (CCC&L) is acknowledged and, in particular, the efforts of Chris Farschon and Sarah Olthof. CCC&L is a nationally known firm specializing in corrosion protection by the use of industrial coatings. CCC&L's corporate laboratory performs product evaluation and quality control services for industrial coatings, as well as environmental analysis for heavy metals. Mr. Farschon and Ms. Olthof participated as members of the Research Team, providing technical consultation on the applications and quality control monitoring of protective coatings undertaken in the industry today, and supervising laboratory services conducted by CCC&L as part of this research.

Additional members of the Research Team who provided critical support throughout the effort included Carlos Montoya, John Curry, Jaime Campo, and Jordan Faltys, of New Mexico State University, and Henry Justus and Matteo Forgione representing Chesner Engineering, P.C.

TABLE OF CONTENTS

LIST OF FIGURES

LIST OF TABLES

EXECUTIVE SUMMARY

Steel structures on current highway bridges, as shown in Figure 1, are typically painted with any of a number of coating systems that employ a zinc-containing primer applied to abrasive blasted steel with epoxy, polyurethane, and/or acrylic topcoats. Structures more than 30 years old were generally painted with lead and chromate alkyd coatings applied over mill scale covered steel.

Regardless of the specific coating type or age, bridge inspection information is needed to determine the condition of a bridge and if any repairs are necessary. The frequency of the inspection and the information gathered during the inspection is defined by the Federal Highway Administration (FHWA) in the National Bridge Inspection Standard (NBIS) guide. Most bridges are inspected every two years. Some bridges are inspected every year due to their condition and design type. A few structures require a more frequent inspection cycle.

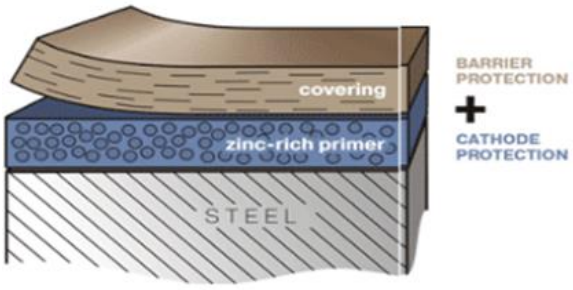

Figure 1 Typical protective cover profile for steel.

Current bridge coating and corrosion evaluation methods generally rely on a combination of "hands-on" and "visual" inspection methods. A hands-on inspection includes both physical and chemical measurements to assess the condition of the coating and substructure. Test methods employed include items such as dry film thickness, adhesion, and surface texture. Where deterioration is observed, samples of the coating and samples of the underlying structure are often scraped off and brought to a laboratory for chemical testing. Where toxic metals are suspected in the pigments, heavy metal laboratory analysis is undertaken on the scraped samples. Varieties of alternative examination methods have been proposed to assist and provide more rapid and quantitative inspection results. Some of these methods include ultrasonic, radiographic, eddy current, electromagnetic acoustic transducer scanning, thermographic, and ground penetrating radar inspection methods. While each of the aforementioned has unique attributes, none of these methods has been reported to satisfactorily discriminate corrosion-related anomalies, and none identify the presence of toxic metals.

The research conducted under NCHRP 164 focused on the development of laser-scanning technology that could provide direct measurement of the condition of the bridge surface and undercoating and assess the level of corrosion, if any, in the underlying steel structure. The concept is based on a laser ablation process where a high-powered laser is focused and fired at a layer of coating, ablating a microgram quantity of mass and inducing a tiny plasma spark. This spark generates an emission of light with a characteristic spectrum. The characteristic of this spectrum depends on the type of coating or condition of the steel. Once the characteristic spectrum is determined for a known coating type or a known level of corrosion, it is possible to match unknown coatings or levels of corrosion to the known spectrum to identify the nature of the unknown sample. The aforementioned technique is a form of pattern matching or fingerprinting.

Using the subject technology commonly referred to a Laser-Induced Breakdown Spectroscopy (LIBS), the research effort focused on five areas of investigation. An outline of the research objectives and findings associated with each respective area of investigation are as follows:

1. Heavy Metals Analysis
    a. Objective:
    Determine the presence of lead (Pb), chromium (Cr), and cadmium (Cd) in paints.
    b. Findings:
    The presence of Pb, Cr, or Cd is readily detectable.

2. Titanium in Paints or Coatings
    a. Objective:
    Measure the titanium dioxide (TiO_2) concentration in paints.
    b. Findings:
    TiO_2 concentration in paints, less than 20%, can be accurately predicted from prepared lab samples.

3. Coating Identification
    a. Objective:
       Identify different types of coatings [epoxy, alkyd, acrylic, latex, urethane, varnish, and Zinc (Zn)-rich primers].
    b. Findings:
       It is possible to distinguish Zn-rich primers and alkyds from other coatings, but the epoxies, acrylics, latexes, urethanes, and varnishes are very similar to each other and were not readily distinguishable during this research effort by the selected approach.

4. Corrosion Indexing
    a. Objective:
       Identify the degree of corrosion on steel structures.
    b. Findings:
       It is possible to distinguish between four grades of corrosion: Rust Grade A, B, C, and D as defined by the Society for Protective Coatings (SSPC) in SSPC VIS-1.

5. Depth Profiling
    a. Objective:
       Develop methods (laser drilling or microdrilling) for depth profiling layers of coating overlying a steel substrate.
    b. Findings:
       The use of a laser to simultaneous drill and induce emission spectra as a depth profiling tool did not provide sufficient precision to characterize and discriminate between layers of coating.
       A new process was developed by the Research Team that combines a microdrilling process and a laser ablation process that can readily distinguish
        - The presence of coatings containing high levels of heavy metals such as Pb, Cr, and Cd;
        - The concentration of TiO_2 in the coating
        - Whether the subsurface coating is from the family of Zn-rich primers or alkyds or some other organic coating.
        - The corrosion grade in the steel as per SSPC VIS-1.
        - The thickness of the layer of coating at 1 mil (25.4 micron) precision.

Since the subject technology generates answers in real time, deployment of such a technology could provide the bridge inspection technician with a tool that generates in the laboratory or in the field, real-time data defining the thickness of the coating, the presence of heavy metals in the coating, and the type of sub-coating corrosion. Such data cannot be detected in real time with conventional inspection techniques.

INTRODUCTION

IDEA Product

The product under development is an automated real-time, quality, steel bridge coating, inspection tool providing the means to characterize the type of surface and subsurface coating(s), the heavy metal and titanium dioxide content in each layer, and the type of corrosion in the steel substrate below the overlying coating(s). The system employs a combined microdrill and a laser to automatically and in sequence etch thin layers (using the microdrill) into the coating material and then analyze successive layers. The microdrill can produce a uniform depression at a pre-set depth into which the laser beam can be directed. Depth profiling resolution is on the order of 1/1000th of an inch or 25.4 microns.

Report Content

The remainder of this report is divided into the following sections. The first section, Concept and Innovation, describes the principles and technical basis of the laser ablation process used in the system and introduces the microdrill concept. The second section, Investigation, summarizes the five research tasks undertaken to provide the

data necessary to demonstrate the viability of the concept for the technology. These tasks include: Heavy Metals Analysis, Titanium Dioxide Content in Coatings, Coating Identification, Corrosion Indexing, and Depth Profiling. The subsequent sections respectively address the Objectives, Research Approach, and Results for each of the aforementioned Research Tasks. These sections are followed by the section outlining the Findings and Conclusions of the effort. The final section, Plans for Implementation, provides a description of the requirements for transitioning the technology to commercial application.

CONCEPT AND INNOVATION

The subject technology employs a rapid laser-scanning technique as a steel bridge coating inspection tool providing the means to characterize the type of surface and subsurface coating(s), the presence of heavy metals and titanium dioxide in each layer of coating, and the extent of steel corrosion below the overlying coating(s). Subsurface coating investigation is commonly referred to as depth profiling. During the course of this investigation, the Research Team developed a new proprietary system, described in greater detail below, for depth profiling through surface and subsurface coatings in one mil increments (1 mil = 0.001 in. = 25.4 microns).

The laser-scanning process is referred to as Laser-Induced Breakdown Spectroscopy (LIBS). In the LIBS process, a very short-duration pulse of energy from a high-power laser is optically focused at a point (e.g., a paint or coating), instantaneously heating the target sample to cause vaporization and atomization of a very small quantity (nanograms) of material within a microplasma. Because of the high plasma temperature (initially >8000 deg K), atoms and ions are electronically excited and upon return to ground state emit light across a broad spectral range (most importantly the range of 200 to 980 nm). The light generated by the plasma is characteristic of the chemical makeup of the ablated material. A schematic showing a general equipment arrangement is shown in Figure 2.

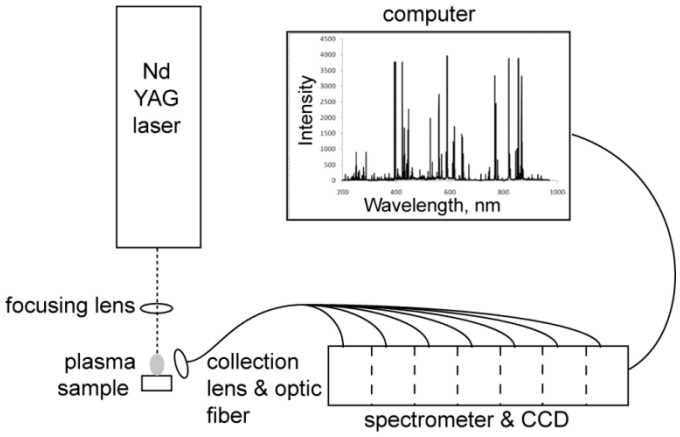

Figure 2 Schematic of laser-induced breakdown spectrometer process.

The Figure 2 schematic shows an Nd-YAG laser [The type of laser used by the Research Team was an Nd-YAG laser (neodymium-doped yttrium aluminum garnet) laser; Nd: $Y_3Al_5O_{12}$ is a crystal that is used as a lasing medium for select solid-state lasers) emitting a power laser beam directed through a focusing lens and onto a test sample for analysis. The high power associated with the laser generates a plasma that emits light that is collected and transported in an optical fiber to a spectrometer and charged coupled detector (CCD). The spectrometer resolves the light into its component wavelengths and the CCD transfers the information electronically to a computer for storage and analysis.

The LIBS process is fundamentally similar to traditional atomic emission spectroscopic (AES) methods that are used for elemental analysis. Each element emits a characteristic set of discrete wavelengths according to its electronic structure. By observing these wavelengths and their respective emission intensities, the elemental composition of the sample can be determined, as shown in Figure 3.

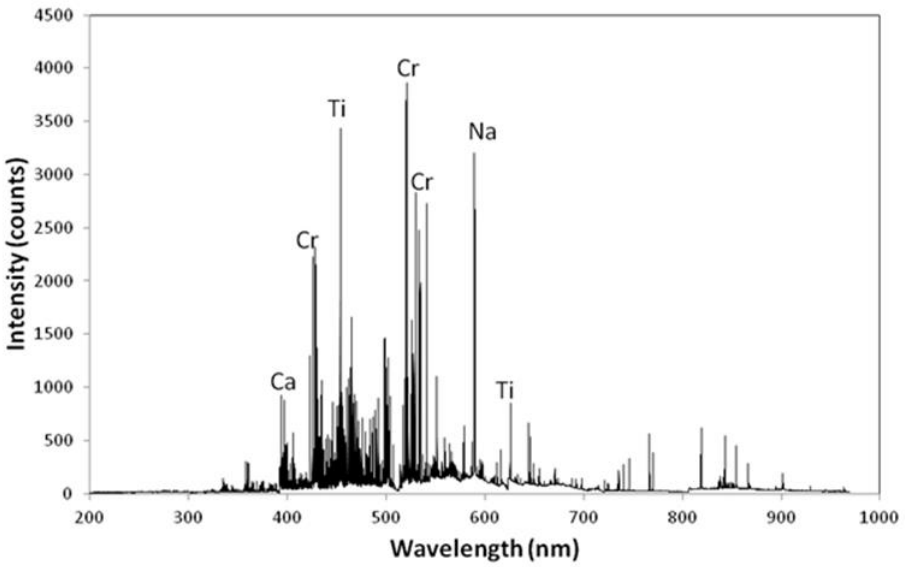

Figure 3 Spectra from paint from the Brightman Street Bridge used in this project, with prominent peaks labeled.

These spectral data can also be used to generate characteristic spectral patterns or fingerprints. These patterns can then be associated with specific paints and coatings, steel and levels of corrosion. With a suitable database of information, the spectral data can then be used to identify the elemental makeup of the target material or the material type or degree of corrosion reflected by the spectral fingerprint.

Using a laser to characterize the properties of paints, coatings, or the degree of corrosion and the newly developed microdrill depth profiling system provides a unique opportunity to provide real-time sensing of painted steel coatings and subsurface steel substrate quality in laboratory or field applications.

INVESTIGATION

Research Objectives

The objectives of this NCHRP 164 research effort were to investigate the feasibility of utilizing LIBS to determine the properties of surface and subsurface coatings and the condition of steel (corrosion) on the underlying steel structure. Five specific tasks were undertaken: (1) Heavy Metals Analysis, (2) Titanium Dioxide Content, (3) Coating Identification, (4) Corrosion Index Development, and (5) Depth Profiling of Coating Subsurface. A listing of these tasks and their respective objectives is provided in Table 1.

TABLE 1
RESEARCH TASKS

Task	Assessment	Objectives
1	Heavy Metals Analysis	Determine the presence or absence of heavy metals (Pb, Cr, and Cd) in paints.
2	Titanium Dioxide (TiO_2) Analysis	Measure the TiO_2 concentration in paints.
3	Coating Identification	Identify different types of coatings in place on structures (epoxy, alkyd, acrylic, latex, urethane, varnish, and Zn-rich).
4	Corrosion Indexing	Identify the degree of corrosion on steel structures.
5	Depth Profiling	Develop methods for drilling into materials, performing all the functions listed above during the drilling process.

1. Heavy Metals Analysis

To properly maintain bridges it is necessary to periodically remove the existing coating and apply new coating systems. While almost all new paints, due to federal and state regulation, are lead (Pb), chromium (Cr), and cadmium (Cd) free, many steel bridges in the highway system are still coated with older paint that contains toxic heavy metal pigments in varying concentrations. As a result, removing paints from older structures through abrasive blast cleaning processes is still a concern. The first step in any coating removal process should therefore be the identification of whether heavy metals are present in the surface or subsurface coatings. The objective of Task 1 was to assess whether the LIBS process could be used to identify presence of Pb, Cr, or Cd in paints and coatings.

2. Titanium in Paints or Coatings

Pigments are additives to the coating formulation that impart specific properties to achieve the desired film properties. The most significant of these properties include color, opacity, viscosity, weather and moisture resistance, corrosion resistance, mildew resistance, and skid or slip resistance. Titanium dioxide (TiO_2) in powder form has excellent light-scattering properties and is used in paints and coatings providing opacity and brightness. It is specified by most transportation agencies in paints and coatings. The objective of Task 2 was to assess whether the LIBS process could be used to identify presence and quantity of TiO_2 in paints or coatings.

3. Coating Identification

Prior to environmental regulations introduced in the late 1980s, the types of coating materials were less numerous and more tolerant of less than optimum surface preparation conditions. This was because paint formulations contained high volatile organics (VOCs) to allow the material to wet or penetrate steel surfaces. The most successful were red lead primers and vinyl resins. Environmental regulations in the late 1980s, however, discouraged the use of these materials. As a result, paint manufacturers reformulated their coatings to comply with new regulations. This led to the development of a wide variety of high-tech coating materials that are much more sensitive to surface preparation and environmental application practices. (Several organizations such as American Society for Testing and Materials, NACE International, and the Society for Protective Coatings have issued consensus standards to minimize surface preparation and application inadequacies.) Some of the more common coating types currently in use include acrylics, alkyds, epoxy (amine, polyamide), inorganic zinc primers, organic zinc primers, polyurethane, and urethane. The objective of Task 3 was to assess whether the LIBS process could be used to distinguish between various coating types.

4. Corrosion Indexing

The primary reason for coating steel is to prevent corrosion. Since current bridge coating and corrosion evaluation methods generally rely on visual inspection methods, subsurface corrosion (below the painted surface), will generally go undetected (Visual inspection methods are defined for painted steel surfaces in ASTM D610, where the type of rusting and the percent coverage over a defined surface area defines the degree of corrosion.) The objective of Task 4 was to assess whether the LIBS process could be used to identify and determine the severity of corrosion on or below the painted surface. Corrosion Indexing is the term used in this report for classifying the degree of corrosion on a steel substrate.

5. Depth Profiling

Modern day coating systems are multilayered. As a result, to determine the type of coatings or the degree of corrosion on an underlying steel substrate requires an analytical technique that can penetrate or depth profile the coating system. In practice, this is usually done by scraping off the coating surface and visually observing the undercoating or removing layers and bringing fragments to a laboratory for analysis. A laser-based system has the potential to provide the means to penetrate and analyze the surface and subsurface of a multilayered coating system. The objective of Task 5 was to assess whether the LIBS process could be integrated into a subsurface depth profiling system to distinguish the coating layers and the presence and degree of corrosion below the coatings.

LIBS Equipment

Two laser systems were used during the research effort. The first laser system, located at New Mexico State University (NMSU), was utilized for the heavy metals, titanium dioxides, coating materials identification, and corrosion indexing assessments. The second system, located at Chesner Engineering (CE) facilities in Massachusetts,

was developed (conceived, designed, and fabricated) during the course of this investigation to provide the means to more accurately depth profile layered coatings. (Initial depth profiling trials were conducted using laser drilling with the laser system at NMSU; however, interferences encountered during testing resulted in the development of a new system.)

The LIBS system used to generate and record the spectra at NMSU consisted of an Nd: YAG 1064 nm 200 mJ laser supplied by Big Sky Laser Technologies, Inc., and an Ocean Optics LIBS 2500-7 channel system spectrometer. This system includes a sample chamber consisting of a sample platform, a focusing lens and a fiber optic cable designed to collect and transmit the light emission from the ablated aggregate to the spectrometer and charged couple device. A photograph of the NMSU LIBS system is shown in Figure 4. The LIBS system used in conjunction with the microdrill for final depth profiling testing was located at CE facilities in Massachusetts. This system consisted of an Nd: YAG 1064 nm 350 mJ laser supplied by Big Sky Laser Technologies, Inc., and an Avantes, AvaSpec-2048/3648 two channel spectrometer. The new (proprietary) system included a specialized testing chamber and rotating sample platform housing a computer-controlled microdrill capable of drilling into the sample in one mil increments. The system provides for alternating drilling to penetrate the sample and laser firing to analyze the content of the surface of the newly drilled depth. A photograph of the microdrill system is shown in Figure 5.

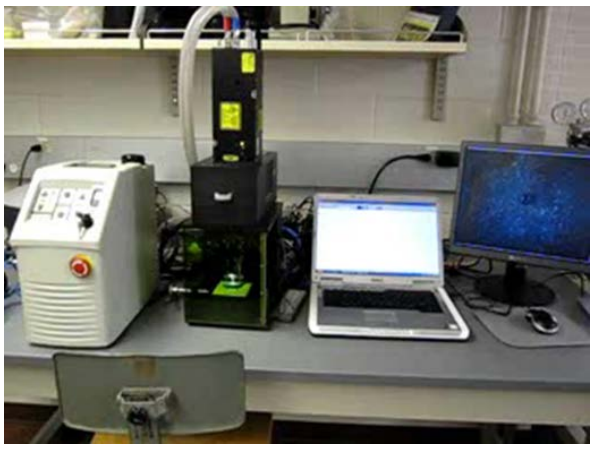

Figure 4 LIBS lab system at New Mexico State University.

Sample Analysis

Laser power and analytical procedures varied slightly for the various applications investigated in this study. In all cases, the laser power was the maximum setting that did not saturate the CCD detector. This produced the maximum amount of information in each spectrum. For applications in which various elements or characteristics were sought (heavy metals analysis, TiO_2 analysis, identification of coatings, and corrosion indexing), multiple spectra were collected from each material and averaged into a single spectrum for modeling (see Chemometric Modeling below). This procedure has two advantages: it minimizes the effect of shot-to-shot variability inherent in LIBS analysis and also minimizes the effect of heterogeneity in the samples. In contrast, single spectra were examined for drilling studies because each laser shot samples a slightly deeper level in the material. Averaging depth profile spectra limits the ability to accurately detect the depth at which the laser encounters a new material.

Chemometric Modeling

Chemometric, or multivariate statistical modeling, was used to analyze the data. This approach makes use of the entire spectral output (not just one wavelength) to pattern match or fingerprint the spectrum of the material in question. This pattern can then be used to identify unknown materials by comparing the unknown material to a database of known materials to determine if a spectra pattern match can be found. Two related multivariate techniques were employed in this analysis: (1) Principal Component Analysis (PCA) and (2) Partial Least Squares Regression (PLS). Both PCA and PLS models were developed using the multivariate statistical program Unscrambler©.

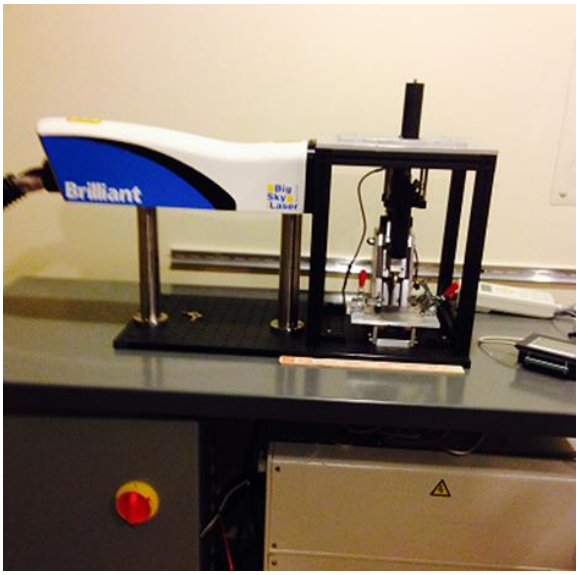

Figure 5 Microdrill technology developed during this study.

PCA is a method used to describe the data. Each laser spectrum contains over 13,000 data points (over 13,000 dimensions), far too many to understand without somehow reducing the amount of information. In PCA, the number of important variables is reduced by calculating linear regressions (principal components) through the multidimensional data set. Principal Component 1 (PC 1) describes most of the variance in the data set. PC 2 is perpendicular to PC 1 and explains significantly less of the variance. Subsequent principal components are all perpendicular to PC1, PC 2, and each other; each PC describes less of the information until they are basically describing the noise in the data set. By combining variables through linear regressions, the number of variables can be reduced from over 13,000 to several. In this report, the Research Team will show only two variables: PC1 and PC 2.

The main result of PCA is a score plot, which is a diagram of PC 1 vs. PC 2. The samples plot on this two-dimensional diagram, which can be interpreted like any two-dimensional (y vs x) diagram. Samples that are similar in composition plot near each other and those with very different compositions will plot in a different section of the diagram. The advantage is that the diagram is only two-dimensional; most of the important information in the spectra is utilized. A two-dimensional diagram is a plot of two variables (*x* and *y*) associated with one or more samples that were previously analyzed. The specific sample magnitude of *x* and *y* defines a point (or vector) in space in this two dimensional diagram for that sample. Samples that have similar x and y variables will generate points (or vectors) that plot close together, while samples with dissimilar variables will plot in different locations. PCA score plots are generating similar points in two-dimensional space; however, the points generated are plotted on multidimensional space vectors (eigenvectors) that represent linear regression lines that pass through the data in multidimensional space. Samples that are similar in composition plot near each other and those with very different compositions will plot in a different section of the diagram.

PLS is similar to PCA but can be used to develop models that can project values (dependent variables) for unknown samples based on previously calibrated data generated from an original data set. The additional dependent variables can be values, such as the weight % TiO_2. In this case, the variables in the spectra that correlate with TiO_2 will be the most important. Like any calibration, once the model is calculated, one can input new spectra and calculate the values of the additional variable (weight % TiO_2 in this example). This process is similar to linear regression analysis with two variables, where a calibrated data set is used as the basis for predicting dependent variables from unknown samples; but in this case the regression is occurring through multidimensional space; not two dimensional space. The additional variables can also be indicator integers. Integers 1 and 0 were commonly used by the Research Team in this investigation to model data in which there are two groups. Integers 1 and 0 were also used to denote dependent variables such as yes and no; or belongs to this group and belongs to some other group. (“Yes”

being set equal 1 and "No" being set equal to 0; or "belongs to group" set equal to 1 and "belongs to some other group," being set equal to 0.)

For models in which it is desirable to separate three or more groups of materials from each other, matching algorithm models were employed. Matching algorithm models represent a series of PLS models, each of which compares one group to all the other groups. This is a form of discriminant analysis. The first model compares the spectrally most distinct material to all of the others. Then that group is eliminated from all subsequent models. The second model compares the next most distinct material to all of the remaining groups, and then that group is eliminated from all subsequent models. In this manner, the materials become more similar to each other as the algorithm develops, but it is possible to distinguish them because they are only compared to each other. This is much like looking at the colors in a painting. It is difficult to distinguish between similar shades of blue when one is looking at all the colors in the painting. However, if one focuses on an area that contains only the shades of blue, the differences between them become apparent.

A total of five different models, listed in Table 2, were developed in this effort. The column labeled "predictor type" in Table 2 lists for each model the type of evaluation procedure used to generate the model output.

TABLE 2
MODEL DEVELOPMENT SUMMARY TABLE

Analysis	Model Reference	Parameter of Interest	Predictor Type	No. of Spectra Averaged
Heavy Metals	Pb-Cr-Cd Models	Pb, Cr, Cd concentrations	Indicator Integer (Yes = 1; No = 0)	20
Titanium	Ti Model	TiO_2 concentrations	Compositional Calibration Curve	20
Coating Identification	Coating Model	Coating Type (i.e., epoxy, alkyd, etc.)	Matching Algorithm Indicator Integer (Yes = 1; No = 0)	50
Corrosion Indexing	Corrosion Model	Corrosion Grade as Specified by SSPC VIS-1	Matching Algorithm Indicator Integer (Yes = 1; No = 0)	50

HEAVY METALS ANALYSIS

Objective

Task 1 of the study was designed to determine if laser spectroscopy could be used to measure the concentrations of Pb, Cr, and Cd in coatings.

Research Approach

Preliminary attempts were made to develop calibration standards with different concentrations of powdered metal dust blended into paint samples (i.e., Cr). The goal was to develop recognizable spectral patterns for predetermined heavy metal concentrations and use these spectra to predict actual levels in unknown paint samples. After several attempts however, it was found to be very difficult to produce homogenous paints, especially at low concentrations. It was important to be able to generate homogeneous (or completely mixed) metal dust with the paints to ensure that the "location" hit by the laser on the paint would not significantly influence the output spectral pattern, defining the heavy metal concentration. The Research Team was not successful in achieving a complete mixing of metal dust with the paint. Thus, the Research Team's focus shifted to a more simple approach: that of distinguishing between samples with heavy metals and those without. This approach turned out to be highly successful.

To conduct this analysis, steel demolition coupons were obtained from the Brightman Street Bridge (these samples were provided by Corrosion Control Consultants and Labs, Kentwood, Michigan.) The Brightman Street Bridge spans the Taunton River in Massachusetts. It opened in 1908 and was closed to vehicular traffic in 2011. Highly

corroded samples, known to contain paints with chromium (Cr), cadmium (Cd) and lead (Pb) concentrations were available from various parts of the bridge. The paints have two colors as shown in Figure 6: a lower red paint and an upper green paint. These paints were selected for Pb, Cr, and Cd analysis.

Figure 6 Section of the Brightman Street Bridge used to detect heavy metals.

Note the older, dark red paint covered by paler green paint.

Laser Analysis and Modeling Procedures: Pb, Cr, and Cd Models

The first step in distinguishing between samples with and without heavy metals was to acquire a robust signal for the heavy metals. Twenty laser-induced spectra were collected from each painted surface; these spectra were averaged into a single spectrum. Emission lines in the spectra with heavy metals (i.e., Pb, Cr, and Cd) were identified by comparing them to the NIST Atomic Spectra Database. Specific Pb, Cr, and Cd frequencies (Pb = 405.8 nm, Cr = 357.9 nm and Cd = 340.4 nm) were used to detect the presence of the respective heavy metals (http://www.nist.gov/pml/data/asd.cfm).

Figures 7–9 show the spectra for Pb, Cr, and Cd, respectively, generated from the green and red paints from the Brightman Street Bridge, compared to modern coating (epoxy and urethane) spectra that contained zero heavy metals. Samples with heavy metals are readily identifiable. In all cases, the green paint had the highest level of heavy metals, the red paint a lower level, and the epoxy and urethane coatings negligible levels.

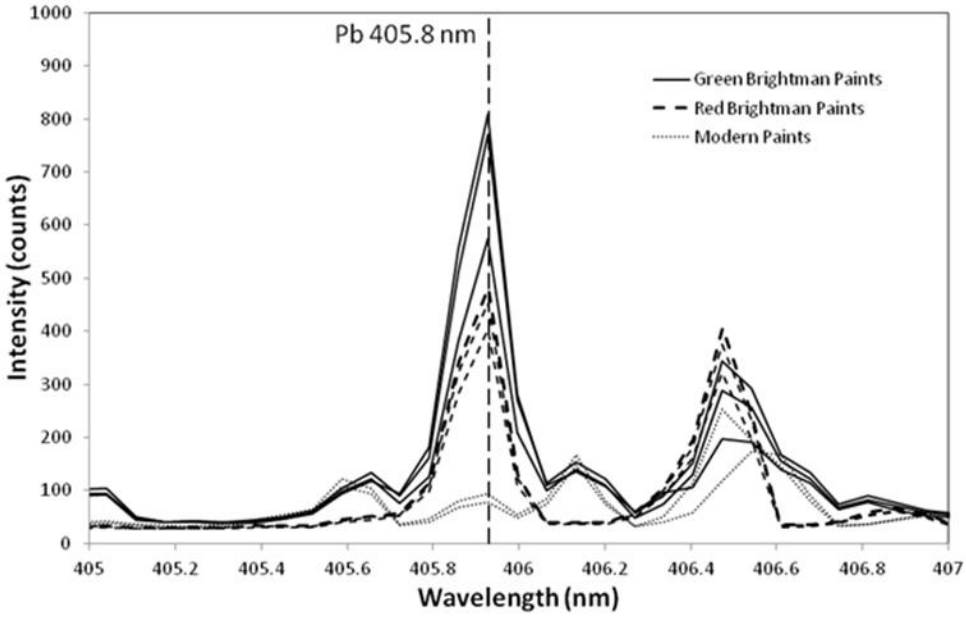

Figure 7 Spectra for the Brightman Street Bridge (green and red paints) and modern coatings. The Pb line is at 405.8 nm.

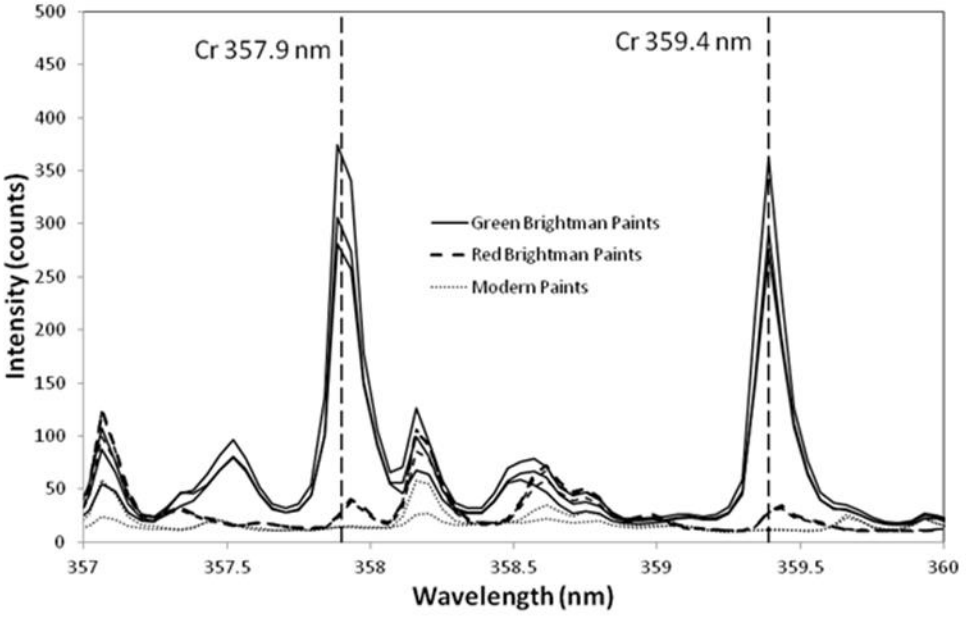

Figure 8 Spectra for the Brightman Street Bridge (green and red paints) and modern coatings. The Cr line is at 357.9 nm.

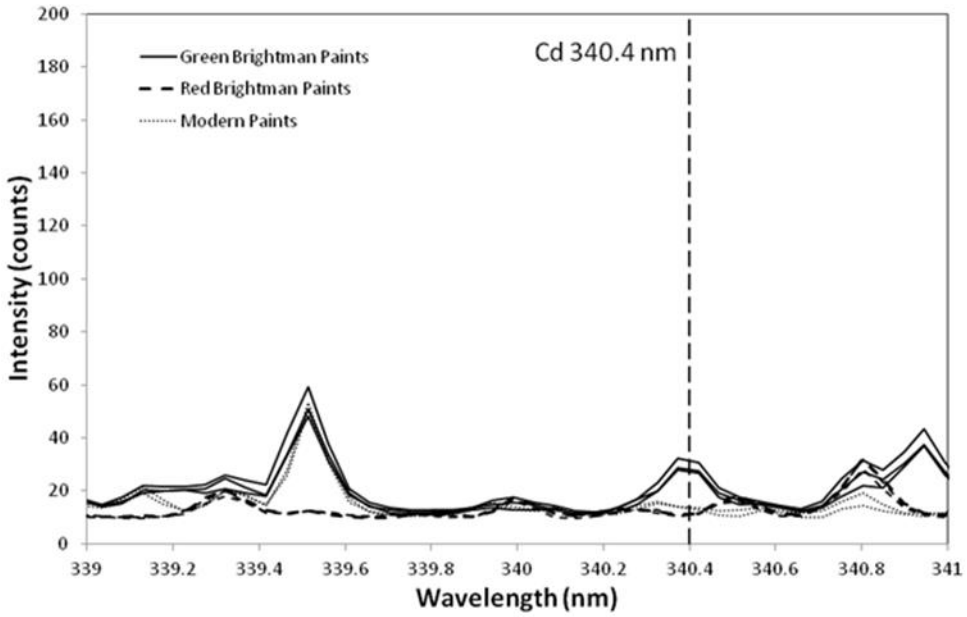

Figure 9 Spectra for the Brightman Street Bridge (green and red paints) and modern coatings.

The Cd line is at 340.4 nm.

A second approach was employed to demonstrate that laser spectroscopy can differentiate between paints with heavy metals and those without. Spectra of the green and red paints from the Brightman Street Bridge and eight modern paints, including alkyds, epoxies, and urethanes, were modeled using PCA. Only the part of the spectra with Pb, Cr, or Cd peaks was used to focus the model on the element of interest. Results are shown in Figures 10–12.

As previously noted, PCA score plots are interpreted in the same manner as other two-variable compositional diagrams: samples that plot near each other have similar compositions and those that plot far apart have different compositions.

In the Pb score plot shown in Figure 10, the Brightman Street Bridge samples plot at high positive values of PC1, and the modern paints plot at negative values. This reflects the high intensities of Pb in the Brightman Street Bridge samples compared to the low intensities in the modern paints.

In the Cr score plot shown in Figure 11, the green paints plot at high positive values of PC, reflecting the high Cr values in the green paint compared to the Brightman Street Bridge red paint and modern paints. Similarly, the Cd score plots, shown in Figure 12, also indicate that the green paint contains higher amounts of Cd compared to the red paint or modern paints.

Clearly, PCA analysis could be used to easily and rapidly distinguish between paints with high concentrations of Pb, Cd, and Cr, and those without.

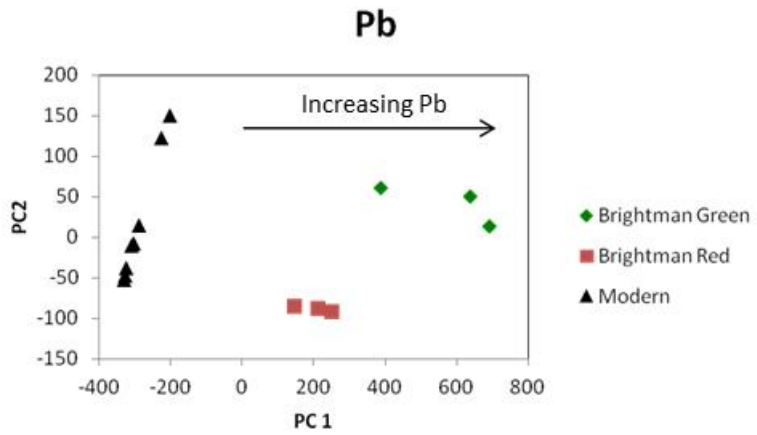

Figure 10 Principal Component Analysis score plot for Pb in paints.

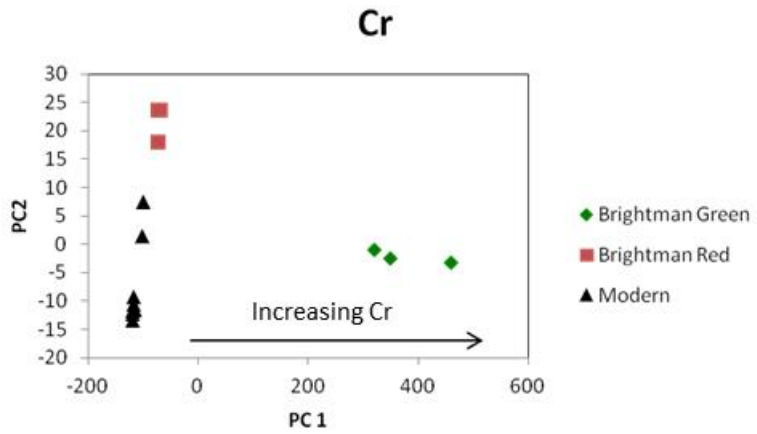

Figure 11 Principal Component Analysis score plot for Cr in paints.

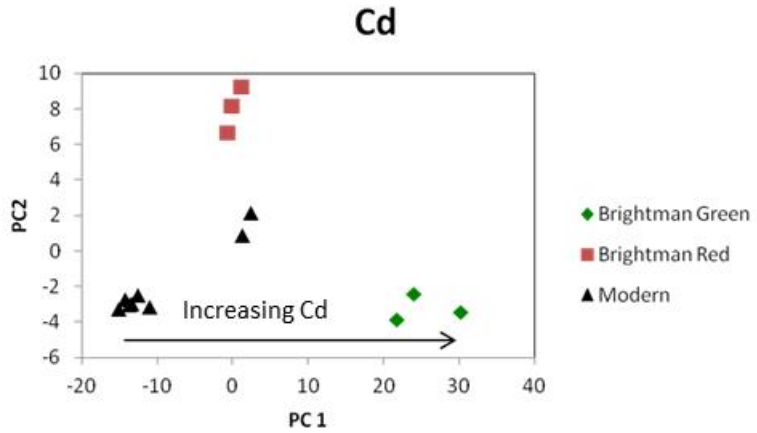

Figure 12 Principal Component Analysis score plot for Cd in paints.

TITANIUM ANALYSIS

Objective

Task 2 of the study was designed to determine if laser spectroscopy could be used to measure the concentrations of titanium in paints.

Research Approach

The general approach employed by the Research Team included the collection of paint samples (Sherwin Williams) with listed titanium dioxide concentrations, verification of those levels in the laboratory using ICP-AES, and determining whether a chemometric model could be developed to predict TiO_2 levels. The chemometric model was developed by correlating the laser-induced spectral data to the measured TiO_2 levels in the test paint samples, using a PLS Regression analysis. The result of this effort is a calibration curve relating model output (spectral fingerprint) to TiO_2 concentration. LIBS research has shown that chemometric (i.e., multivariate) models perform better than traditional univariate models (i.e., correlating the peak area to intensity). This is because of the complexity of the LIBS signal, the intense interactions between all of the atomic particles in the plasma, and the matrix effect in LIBS analysis.

Four paints were purchased from Sherwin Williams for this task, and 50:50 mixes were made of some of them, to create a range in compositions (test samples) from 0 to 21weight % TiO_2 (seven samples were generated for subsequent evaluation and these samples are listed in Table 4). A listing of TiO_2 concentrations in the original four samples is presented in Table 3.

TABLE 3
PAINTS USED FOR TITANIUM CALIBRATION IN THIS STUDY

Paint	TiO_2 concentration
Ultra Deep	0 wt%
Deep Base	4 wt%
Extra White	13 wt%
Luminous White	21 wt%

As listed in Table 4, the absolute values of the Sherwin Williams reported concentrations differ from those in the same paint samples analyzed by ICP-MS (ICP-AES analyses were conducted by Corrosion Control Consultants & Labs, Inc.at their laboratory facilities located in Kentwood, Michigan). As shown in Figure 13, the measured and reported concentrations are, however, proportional to each other; the difference is due to loss of volatiles during drying. Concentrations by ICP-AES were determined by dissolving dried paint specimens. The ICP-AES measured values listed in Table 4 (Column C) were used in the model calibration described below because both the ICP-AES and LIBS measurements were taken on dried paint samples.

TABLE 4
TIO_2 CONCENTRATIONS IN SAMPLES USED IN THE TIO_2 CALIBRATION STUDY

A. Paint	B. TiO_2 Sherwin Williams	C. TiO_2 by ICP-MS CCC&L	D. TiO_2 Measured in This Study
1. Ultra Deep	0	0	-0.9
2. 50 UD + 50 DB	2	4.5	5.3
3. Deep Base	4	9.4	4.7
4. 50 DB + 50 EW	8.5	15.0	16.6
5. Extra White	13	21.0	18.2
6. 50 EW + 50 LUM	17	27.0	—
7. Luminous White	21	33.0	—

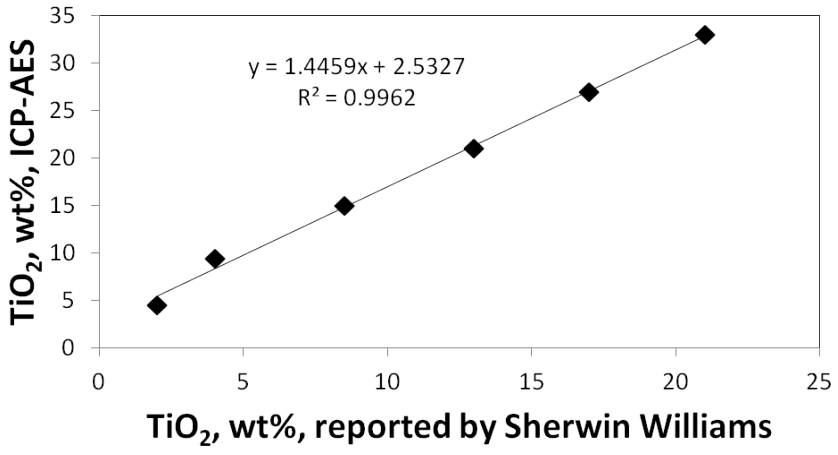

Figure 14 Comparison of reported and measured TiO_2 concentrations in Sherwin Williams paints.

Laser Analysis Modeling Procedures: Titanium Dioxide Model

Twenty laser-induced spectra were collected from each test sample; these spectra were averaged into a single spectrum. TiO_2 concentrations were modeled using Partial Least Squares (PLS) Regression. During the development and analysis of the PLS models, it became apparent that TiO_2 concentrations could be accurately modeled, if TiO_2 levels in the paints were less than 20%, but could not be accurately modeled if the TiO_2 levels were greater than 20%. Since the number of samples is fairly low (five), a series of five calibration curves were calculated. Each calibration was based on four of the samples, and was used to calculate the concentration of TiO_2 in the fifth sample. This "leave-one-out" modeling technique is commonly used in spectroscopy with small sample sets. It is fairly rigorous because the sample being analyzed is not used in each calibration.

The modeled TiO_2 values are listed in Column D of Table 4 and plotted in Figure 14. The correlation is very good, with $r^2 = 0.942$. Since in most instances steel paints will contain less than 20% TiO_2, these results suggest that laser spectroscopy can be used to analyze TiO_2 concentrations in coatings.

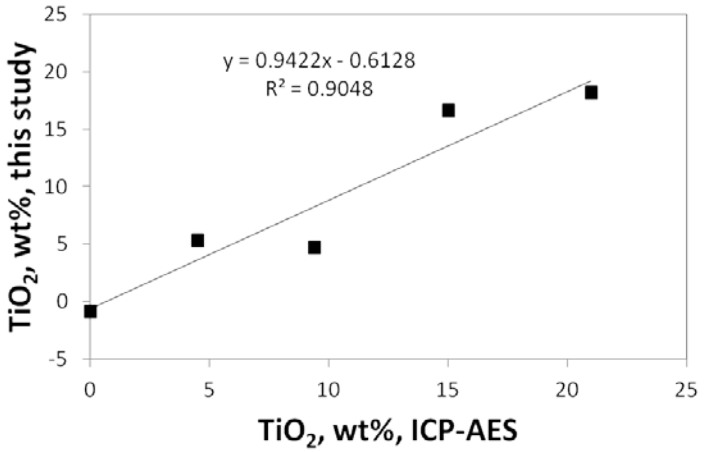

Figure 14 Results of TiO_2 analysis in this study compared with known values as analyzed by ICP-AES at CCC&L.

It is interesting that TiO_2 analysis is inaccurate for TiO_2 concentrations above 20%. The Research Team

speculates that this is a matrix effect, that is, at high concentrations of TiO_2, the titanium and the organic base interact in the LIBS plasma in a different manner than they do at lower TiO_2 concentrations. The solution of this problem is beyond the scope of this pilot study, but suggests an interesting avenue for further research.

COATING IDENTIFICATION ANALYSIS

Objective

Task 3 of the study was designed to determine if laser spectroscopy could be used to determine the type of coating present on a painted steel surface.

Research Approach

The general approach developed included the collection of coating samples that could be laser-scanned to generate a database of spectral fingerprints that could subsequently be used to identify unknown coating samples. A set of 49 coatings, listed in Table 5, were supplied by CCC&L and analyzed in this study. The sample set includes three acrylics, 16 alkyds, 12 epoxies, four latexes, four urethanes, four varnishes, and six Zn-rich paints.

Laser Analysis and Modeling Procedures: Coating Model

The Coating Model employed the matching algorithm technique. Laser-induced spectra from the 49 coatings, listed in Table 5, were generated. Fifty laser-induced spectra were collected from each coating sample and each of these spectra was averaged into a single spectrum.

Initial attempts to model the data were frustrated by the presence of abundant TiO_2 in some coatings but not others. TiO_2 is an additive to coatings, but concentrations of TiO_2 vary by an order of magnitude. Thus, the differences in TiO_2 concentration among the coatings used in this study overwhelmed the signal from the coating materials themselves; early models separated samples by TiO_2 content. The solution to this problem was to eliminate Ti peaks from the spectra. However, because there are 264 peaks of Ti listed in NIST's *Handbook of Basic Atomic Spectroscopic Data*, elimination of all 264 peaks also eliminated valuable information about other elements in the spectra. Thus, all peaks with intensities typically 1% or more of the intensity of the highest peak (108 peaks) were eliminated, leaving only the minor peaks of Ti.

The Coatings Matching Algorithm Model shows that it is possible to separate the Zn-rich primers and alkyds from other coatings, but that the epoxies, acrylics, latexes, urethanes, and varnishes are very similar to each other and were not readily distinguishable by the selected approach.

The algorithm is shown schematically in Figure 15. The schematic illustrates how the Matching Algorithm Model works. In Model 1, an unknown sample is analyzed to determine if its spectral fingerprint matches the fingerprint of a Zn-rich primer. The output will either be Yes or No. If the match occurs (output = yes), the unknown sample is a Zn-primer. If it does not (output = no), the spectra is analyzed by Model 2. In Model 2, the spectral fingerprint is analyzed to see if it matches that of an alkyd coating. The output again will be Yes or No.

TABLE 5
COATINGS USED IN THIS STUDY

Coating Description	Type
Intercryl 520 Off White	Acrylic
Intercryl 520 Black Paint	Acrylic
Intercryl 520 Fawn Paint	Acrylic
Interlac 800 Woodland Night	Alkyd
Primer -Red	Alkyd
Interlac 800 Black	Alkyd
Interlac 800 Red	Alkyd
Interlac 800 Gray Paint	Alkyd
Interlac 800 Safety Yellow	Alkyd
Interlac 800 Safety Red Paint	Alkyd
Interprime 234 Gray Paint	Alkyd
Interlac 800 Black Paint	Alkyd
Interlac 800 Woodland Night Paint	Alkyd
Interlac 800 Black Paint	Alkyd
Interlac 800 White Paint	Alkyd
Interlac 800 Lido Beige Paint	Alkyd
Yellow alkyd paint	Alkyd
Interlac 800 Gray Paint	Alkyd
Interprime 234 red primer	Alkyd
Macropoxy 646 Fast Cure Epoxy: Mill White	Epoxy
Interseal 670HS	Epoxy
Macropoxy 920 PrePrime Epoxy	Epoxy
Safety-Yellow Floor Paint	Epoxy
Zero VOC WB Epoxy	Epoxy
Macropoxy 646, Mill White	Epoxy
Macropoxy 646, Mill White	Epoxy
Interseal 670 HS	Epoxy
Santille 755	Epoxy
Carboguard Gray	Epoxy
Interseal 670 HS	Epoxy
Carboguard White	Epoxy
Latex White Primer	Latex
Traffic Yellow Latex	Latex
White Latex Primer	Latex
Silver White Latex Paint	Latex
2K Urethane Beige Primer-Part 1	Urethane
Anti Graffiti 2K WB Urethane	Urethane
Urethane	Urethane
Carbothan Gray Urethane	Urethane
Red Varnish	Varnish
Insulating Varnish	Varnish
Red Varnish	Varnish
Insulating varnish	Varnish
M-29-1 Series 3500 Zinc Dust Primer	Zn-rich
Carbozinc 11 HS Base Green	Zn-rich
Zinc Clad III Zn-rich Epoxy	Zn-rich
Carbozinc 22 HS, Zinc filler Type II	Zn-rich
Carbozinc Green Epoxy	Zn-rich
Carbozinc Epoxy	Zn-rich

The Matching Algorithm Model Calibration was undertaken by selecting half of the samples for calibrating the model. The remaining half of the samples was used for validating the model. Validation samples were not used in the model calibration. Model 1 was calibrated by dividing the spectra into two groups: Group 1 = Zn rich primer and Group 2 = all other types of coatings. During calibration, the spectra from calibration Zn-primer samples (Group 1) were assigned a value of 1and all other calibration samples (Group 2) a value of zero (the values 1 and 0 represent the dependent variables). As part of the model calibration process, the two groups were separated by a Value of Apparent Distinction (VAD), which is the value set that best separates the two groups. The VAD is set based on the data in the calibration model, and then applied to the data in the validation. Because the samples used in calibration and validation are different, the VAD sometimes does not appear to be the best fit to the validation data. However, if these processes were commercialized, the calibration model would be built on hundreds or thousands of samples, and the calibration would accurately reflect the variation in the unknowns analyzed. The Model 1 VAD value was set at 0.4.

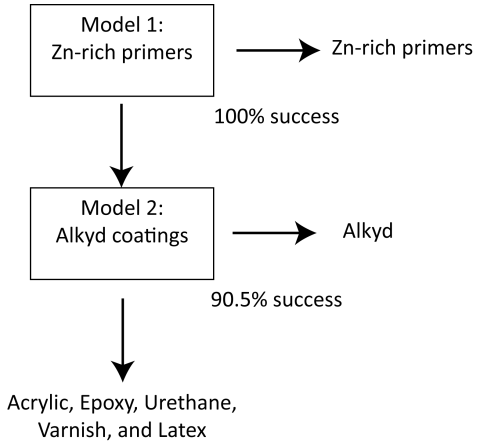

Figure 15 Matching algorithm used in the Coatings Model.

Model validation was tested by introducing the remaining half of the samples (left out of the calibration) into the model to determine how well the model would predict the correct answer ("Is the unknown a Zn primer or Not?"). Those samples with modeled values greater than 0.4 were identified as Zn-rich primers (Group 1) and those samples with modeled values less than 0.4 were identified as all other samples (Group 2). The results are presented in Figure 16. In Model 1, shown in Figure 16, all 24 samples are correctly identified, resulting in a 100% success rate.

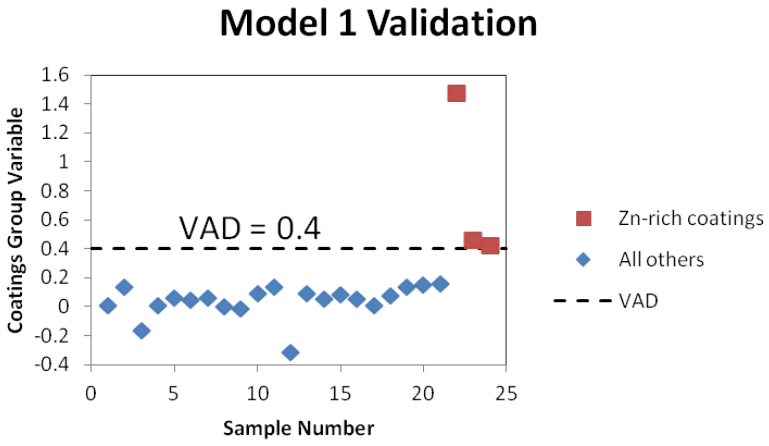

Figure 16 Validation diagram for Model 1 in the Coating Matching Algorithm.

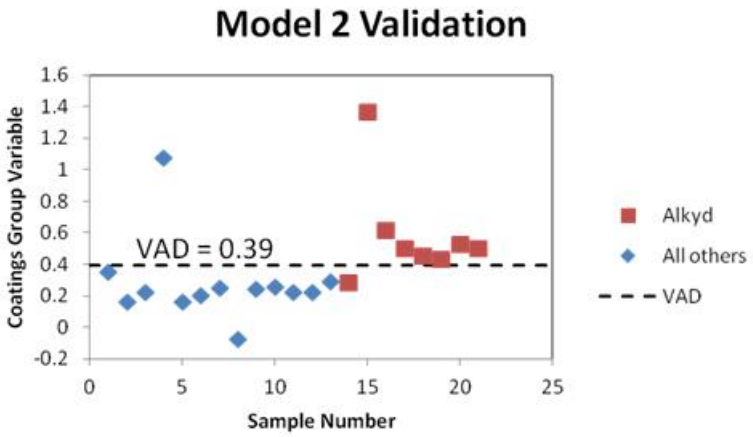

Figure 17 Validation diagram for Model 2 in the Coating Matching Algorithm.

The second model was 90.5% successful at distinguishing between alkyd coatings and the remaining groups. This is shown in Figure 17. Two samples, one alkyd and one epoxy, are incorrectly identified.

The remaining groups of coatings are acrylic, epoxy, latex, urethane, and varnish. These groups were not distinguishable using this method. Reasons for this may be: (1) the continuing effect of abundant Ti in some of the spectra may skew the models; (2) the effect of elements added to color coatings may have a larger effect than the composition of the base coating material; or (3) the coating materials may be too similar to distinguish. Modeling the C/H, C/O, and O/H ratios in the coatings may be a possible method for distinguishing between coatings; however, this necessitates analysis in an environment free of C, H, and O. This is possible in laboratory by filling the sample chamber with Argon (Ar) during analysis, but increases the complexity of field analysis. Additional spectral analysis beyond this study would be needed to attempt to resolve the remaining coating types.

CORROSION INDEXING

Objective

Task 4 of the study was designed to determine if laser spectroscopy could be used to identify the presence and degree of corrosion present on a steel surface.

Research Approach

The general approach employed by the Research Team included the collection of corroded steel samples, the classification of the degree of corrosion (corrosion indexing) associated with each of the samples, the generation of laser-induced spectra for each type of corrosion, modeling of these spectra using a PLS Regression analysis, and the validation of the developed models. X-Ray Diffraction (XRD) analysis was also performed on each sample to establish whether variation in mineralogy could be correlated with corrosion level.

The purpose for classifying or indexing the degree of corrosion was to provide a means to match and calibrate the laser-induced spectra to previously defined levels of corrosion. Corrosion inspection for painted steel surfaces is typically undertaken in accordance with ASTM D610, where the type of rusting and the percent coverage over a defined surface area defines the degree of corrosion. This visual inspection method quantifies the severity of corrosion based on percent coverage rather than severity of the rusted surface.

To define the presence and degree or severity of corrosion, the Research Team selected the approach established by the Society for Protective Coatings (SSPC), as defined in SSPC VIS-1 Surface Cleanliness

Guide. This guide is used to determine the estimated level of surface cleanliness based on the condition of the steel before cleaning. The SSPC VIS 1 visual guide defines four initial conditions (grades of raw steel) that could be encountered prior to abrasive cleaning. These include:

- Rust Grade A: Steel surface covered completely with adherent mill scale and with little if any rust.
- Rust Grade B: Steel surface which has begun to rust and from which the mill scale has begun to flake.
- Rust Grade C: Steel surface on which the mill scale has rusted away or from which it can be scraped, but with little pitting visible to the naked eye.
- Rust Grade D: Steel surface on which the mill scale has rusted away and on which considerable pitting is visible to the naked eye.

Two sets of steel samples were used in the analysis; each of the corroded samples subjected to laser analysis were classified as Rust Grade B, C, or D. One set was from the Brightman Street Bridge, shown in Figure 18, and the second set was collected in a scrap metal yard in Las Cruces, NM, shown in Figures 19 and 20.

Selected laser target locations on each of the samples from the Brightman Street Bridge and New Mexico were given corrosion ratings based on SPCC-VIS-1. These ratings are listed in Table 6.

TABLE 6
RUST GRADE RATINGS FOR CORROSION SAMPLES USED IN THIS STUDY[1]

Sample	Corrosion Level
Brightman Street Bridge, Figure 18	C, D
NM1 (A through L), Figure 19	B
NM3 (A through E), Figure 20	C, D

[1]Sample NM1 was a metal bowl street lamp and Sample NM3 was an electrical box. A third sample NM2, a metal coupling for irrigation pipes, was also collected. It was not used because there was so much bonding material on the surfaces that it was difficult to find rust accumulations that were in locations that the Research Team could analyze.

Figure 18 Corrosion samples used from the Brightman Street Bridge.

Figure 19 Sample NM1 used in corrosion study.

Figure 20 Samples NM3 used in corrosion study.

Laser Analysis and Modeling Procedures: Corrosion Severity Model

Brightman Bridge samples were laser-analyzed in multiple locations, noted with letters in the sample name in Table 7 (7A through 7E). Samples NM1 and NM3, also listed in Table 7, were cut into several sections (samples NM1B to NM1L). Sample NM3 was cut into samples NM3B to NM3E. One sample, NM3C, contained areas with Grade C corrosion and others with Grade D corrosion. These are labeled NM3C_C and NM3C_D, respectively.

Fifty laser-induced spectra were collected from each test location and each of these spectra were averaged into a single spectrum.

XRD analysis was performed to establish whether variation in mineralogy could be correlated with corrosion level. Areas of corrosion were sanded off of the steel with corundum-based sand paper. The powders were collected and analyzed on a Rigaku MiniFlex-II X-ray diffractormeter at New Mexico State University using Cu Kα X-rays. D-spacings were calculated using Bragg's Law and compared to the JCPDS Power Diffraction File listings for inorganic phases. Results are also presented in Table 7. No obvious relationship between mineralogy and grade of corrosion could be determined. Thus, efforts to relate the laser spectra to mineralogy were abandoned.

TABLE 7
RESULTS OF XRD STUDY OF CORROSION SAMPLES[1]

Sample	Corrosion Grade	Maghemite or Magnetite	Hematite	Goethite	Lepidocrocite	Akaganeite	Wustite	Iron	Calcite
NM1B	**B**	X	X	X		X	X	X	X
NM1C	**B**	X	X	X	X	X	X	X	X
NM1D	**B**	X	X	X	X	X	X		X
NM1E	**B**	X	X	X			X	X	
NM1F	**B**	X	X		X	X	X		X
NM1G	**B**	X	X		X	X	X	X	
NM1H	**B**	X	X		X	X	X	X	X
NM1I	**B**	X	X	X	X	X	X	X	X
NM1J	**B**	X	X		X	X	X	X	X
NM1K	**B**	X	X		X	X	X	X	X
NM1L	**B**	X	X		X	X		X	X
7A	**C**	X			X		X	X	X
7B	**C**	X	X	X	X	X	X	X	
7C	**C**	X	X		X	X	X	X	
NM3B	**C**	X	X	X		X	X		X
NM3D	**C**	X		X	X			X	X
NM3C_C	**C**	X	X	X	X	X	X	X	
7E	**D**	X	X	X	X	X	X	X	X
NM3C_D	**D**	X	X	X	X	X	X	X	X
NM3E	**D**	X	X	X	X	X	X	X	X
7D	**D**	X	X		X	X	X	X	X

[1]An X indicates that the phase is present in the sample.

PCA modeling and PLS models were used to determine whether the spectral data could be sorted out and correlated to the three levels of Corrosion (Levels B, C, and D). The data were first analyzed using PCA.

The PCA score plot is shown in Figure 21. The results show that the three types of corrosion are fairly distinct from each other. Corrosion Level C samples split into two groups; one group is from the Brightman Street Bridge and the other from the New Mexico samples. However, as demonstrated below, the samples can be modeled successfully as a single group. This suggests that the models may be independent of location (i.e., whether the corroded samples came from the Brightman Street Bridge or New Mexico).

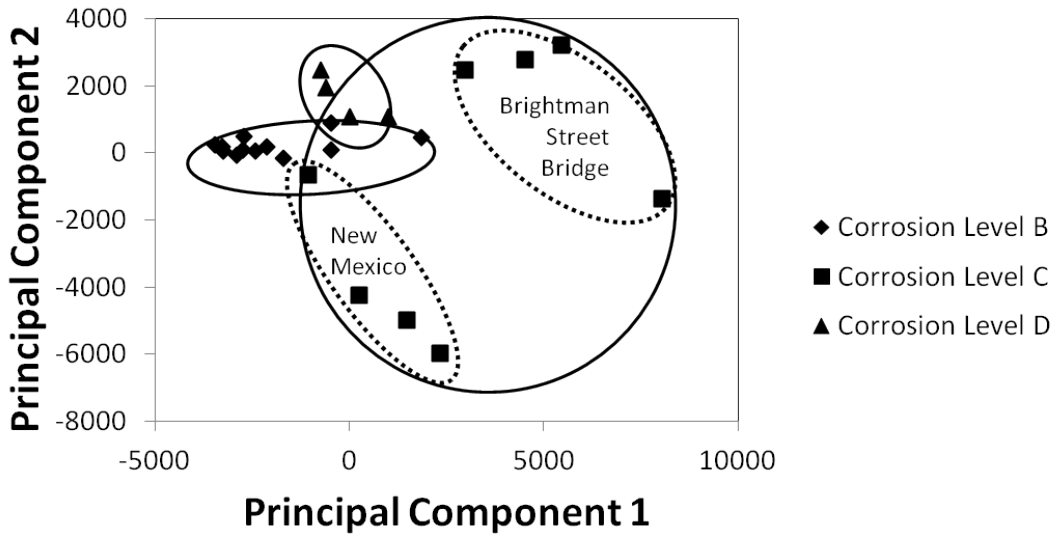

Figure 21 Principal Component Analysis score plot for corrosion samples used in this study.

The Research Team developed a matching algorithm to distinguish Grades of Corrosion, in a manner similar to the Coating Model in the previous section. The matching algorithm was developed with half of the samples of each grade, and then validated with the other half of the samples. The algorithm developed for analysis of Corrosion Levels is presented in Figure 22. Model 1 compares Level C corrosion to Levels B and D (grouped together). Having been identified in Model 1, Level C samples were left out of further models. Model 2 compares Level D corrosion to Level B corrosion.

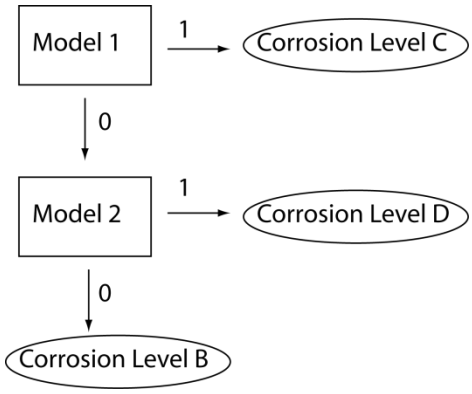

Figure 22 Algorithm for analysis of corrosion levels. The algorithm consists of two PLSR models. Each model compares two groups of materials.

In Model 1, Corrosion Level C samples were assigned the value 1; samples of Levels B and D were assigned the value 0. Using half the samples, a model was constructed that distinguishes between the spectra of the two groups. The VAD (Value of Apparent Distinction) was chosen that separates the two groups; in this case, the VAD = 0.58. The remaining spectra (from the samples left out of the calibration) were then entered into the model, and integer variables were calculated. These results are shown in Figure 23, Part A. One sample from the Level C group was misclassified as a Level B or D sample, resulting in a success rate of 92%.

Because Corrosion Level C was successfully identified in Model 1, all Level C samples were eliminated from Model 2, which distinguishes Level B from Level D corrosion. Here, Level D samples were assigned the integer variable value of 1 and Level B samples were assigned 0. The model was again calibrated with half of the samples, and a VAD of 0.4 was chosen. The results of running the validation samples through the model are shown in Figure 23, Part B. Here, one Level D sample was misclassified, resulting in an overall success rate of 88%.

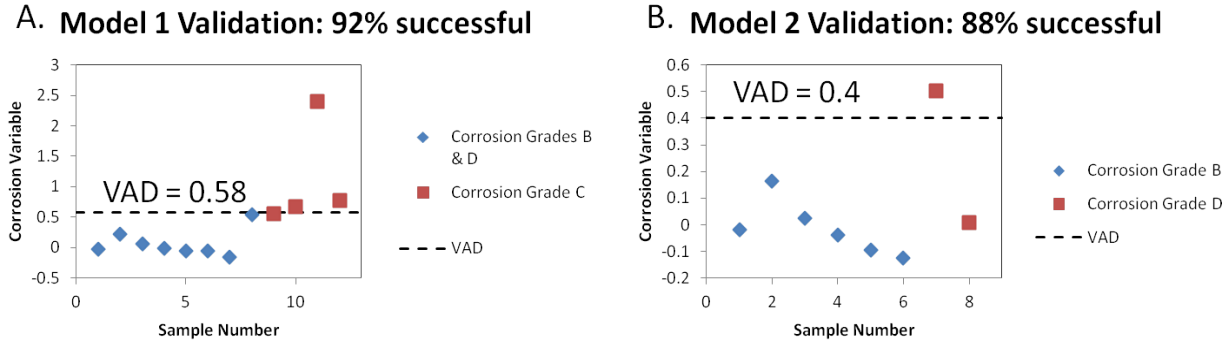

Figure 23 Results of models in the Corrosion Grades algorithm.

This analysis and modeling technique strongly suggests that corrosion indexing (i.e., different levels of corrosion) can be achieved using laser spectroscopy.

DEPTH PROFILING ANALYSIS

Objectives

Task 5 of the study was designed to determine if laser spectroscopy could be used to depth profile multilayered coatings and paints on a steel substrate.

Research Approach

The original idea in this work was to use the laser to drill holes through layered materials. The material at the bottom of the hole would be ablated and analyzed, providing simultaneous drilling and analysis. This method has been reported widely in the literature; however, the depth resolution (the precision to which one can measure the depth to a layer boundary) is poor in all studies except those with very thin layers. The amount of contamination of laser spectra during laser drilling has been shown to be proportional to the thickness of the layer.

During this research effort, spectral contamination was recorded even in very thin layers. It was hypothesized that during laser drilling the walls of the hole drilled by the laser are not smooth and uniform, but jagged with many overhangs. As a result, the laser ablates the overhanging material as well as the material at the bottom of the hole, resulting in spectra that are contaminated by all of the materials above the laser shot (These results were presented in the Stage 1 report for NCHRP 164). In addition, assessing the depth of penetration, using a laser drill, was found to be a secondary issue. Since the penetration distance for any laser shot is dependent on the material through which the laser drill is penetrating and since this material is unknown at the time of drilling, it is difficult to determine the exact depth of penetration of a laser drill at any point in the drilling process. This was also deemed to be problematic. The penetration depth in a laser drill is based on the number of laser shots at a specific location and the known penetration distance per shot previously calibrated. The difficulty stems from the fact that layered materials will have different penetration rates per laser shot. For example, a laser shot at a given power will penetrate an epoxy much deeper than a Zn-rich primer.

To remedy this situation, the Research Team undertook the development of a new laser-drilling system that would (1) eliminate any cross contamination between layers, and (2) provide a system that could positively penetrate

to a predetermined depth, and do so in very fine increments, on the order of paint coating film thicknesses. The proprietary invention, developed during this effort, makes use of combined microdrill and a laser to automatically and in sequence etch thin layers (using the microdrill) into the target material and then analyze the flat bottom surface of the depression with the laser. The microdrill can produce a uniform depression at a pre-set depth into which the laser beam could be directed. Depth profiling resolution is on the order of 1/1000th of an inch or 25.4 microns. Because the diameter of the depression is much larger than the laser beam, the contamination phenomena is eliminated, making it possible to analyze a true depth profile. Automatic computer-controlled sequential drilling and laser firing results in rapid penetration of coating depths.

Layered coupons supplied by CCC&L were used to investigate and compare the effectiveness of a laser drill alone and the microdrill-laser system to resolve layers of coating in a multilayered coupon. The coupons were all identical except for the color of some paint layers, and were created for the Driscoll Memorial Bridge repainting project (NJTA Project 100.185.1). A description of the coupon layers is provided in Table 8 and a cross section of the coupon is shown in Figure 24.

TABLE 8
LAYERED COUPONS USED FOR DRILLING STUDIES

Layer ID	Layer Description	Layer Color	Photo of top view of coupon
Layer E	Acrolon 218 HS Acrylic Polyurethane Gloss	Federal Spec color: 14672	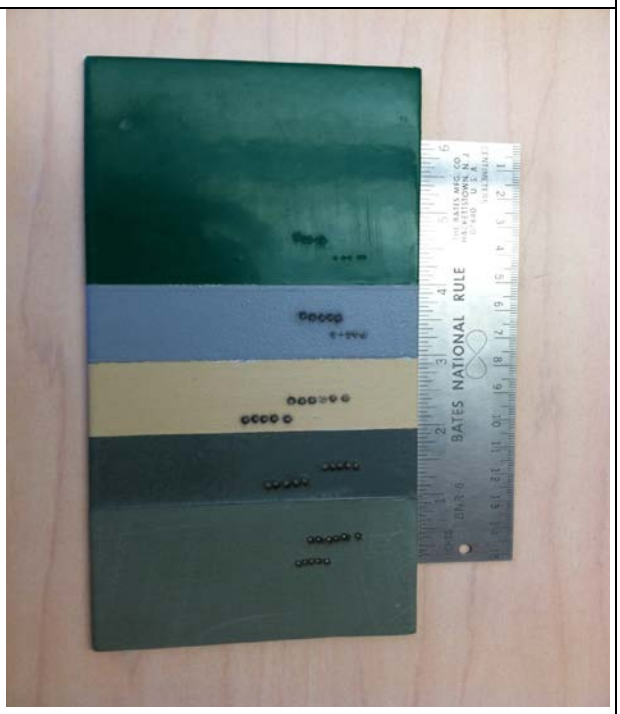
Layer D	Macropoxy 646 Fast Cure Epoxy	SW 4026 Slate Gray	
Layer C	Macropoxy 646 Fast Cure Epoxy	SW 4003 Pallet Tan	
Layer B	Macropoxy 920 Pre-Prime Epoxy Pre-Primer	gray	
Layer A	Zinc Clad III HS, Organic Zinc-rich Epoxy Primer	dark gray	

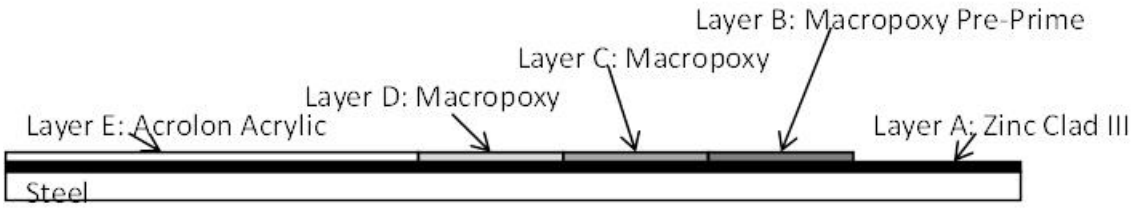

Figure 24 Cross section of layered coupon used in this study.

Laser Analysis and Modeling Procedures

Multilayered coupons, described in Table 8 and depicted in Figure 24, were used in this study to compare spectra produced with the microdrill to those produced by laser drilling. Layer B (two layers over steel) and Layer C (two layers over steel) were analyzed by both techniques.

Drilling through Layer B

Spectra produced by laser drilling for Layer B are presented in Figure 25. Only every tenth spectra is presented because of space limitations on a single diagram; 160 spectra were acquired in this depth profile. Every tenth spectra means that the data presented are only showing the results of every tenth laser shot into the hole being drilled by the laser. Examination of every tenth spectrum should also make the changes between layers look more abrupt, not more gradual. One would expect to see a change in spectra as the laser drills from the top Macropoxy Pre-Prime coating through the Zn-clad and finally into the steel layer. For laser drilling, this was not the case. The spectra look very similar to each other, with only small changes with depth. The three large peaks between 450 nm and 500 nm are the Zn peaks at 468.0, 472.2, and 481.0 nm, and they persist to the bottom of the hole, although visible inspection revealed that the drill hole penetrated steel. The first laser shot contains significant levels of sodium (Na), probably due to surface contamination (technician fingerprints). Na is present everywhere on the surface of all materials that have been handled by humans. Na was not observed in the microdrill spectra because the two channel spectrometer used for the microdrill did not cover the range of wavelengths of Na light.

The cross section to the right of the spectra shows the layers of Macropoxy Pre-Primer, Zinc Clad III, and steel that should be discerned in the spectra. No clear spectral differences with depth exist, and it is impossible to identify the boundary between layers from the spectral data.

In contrast, spectra produced by the microdrill for Layer B are presented in Figure 26. All spectra are presented. The major difference between the microdrill spectra and the laser drill spectra is the clear difference in spectra with depth. This is because the microdrill drills a hole with a much larger diameter than the laser beam. Thus, the laser cleanly samples the material at the bottom of the hole without the contamination that is evident during laser drilling. The microdrill drill bit used in this research was a 2 flute center cutting 3/16 in. endmill.

The first spectrum produced while using the microdrill in Layer B, shown in Figure 26, shows intense Zn peaks, which is not expected for the coating of Macropoxy Pre-Primer. However, in this case the technician erroneously drilled before taking a laser shot. Thus, the first layer sampled by the laser was Zinc Clad III. Zinc Clad III extends down through spectrum 11. Spectrum 12 represents steel, with Fe peaks but no Zn peaks. The lack of Zn peaks in spectra from the underlying steel is important, because Zn has a low melting point and is easily mobilized by the laser plasma. Thus, these data indicate that use of the microdrill effectively eliminates the contamination issue inherent in laser drilling.

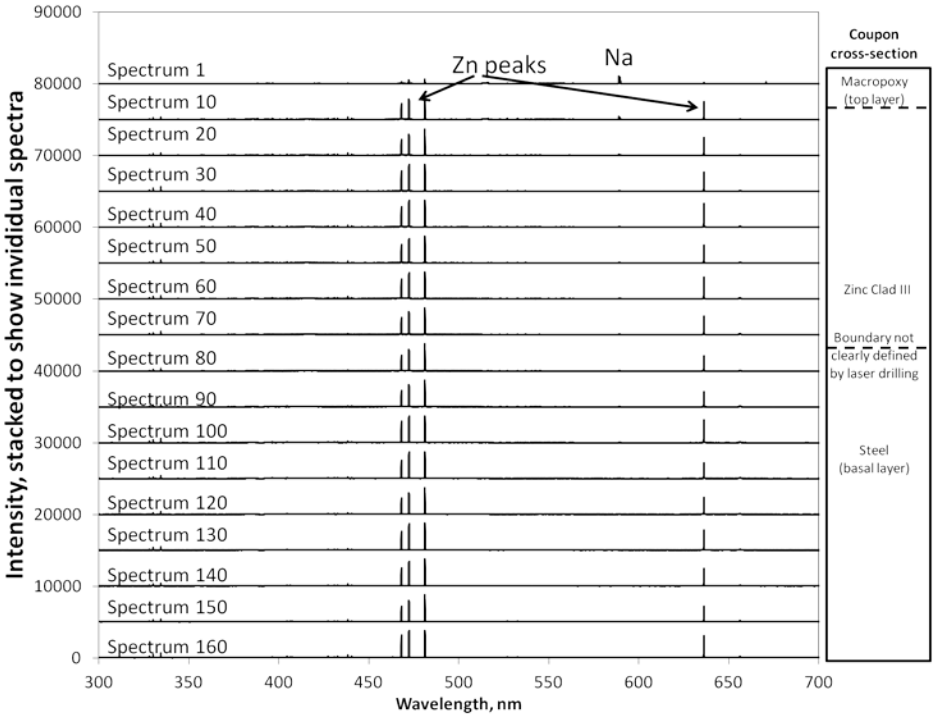

Figure 25 Spectra from Layer B produced by laser drilling.

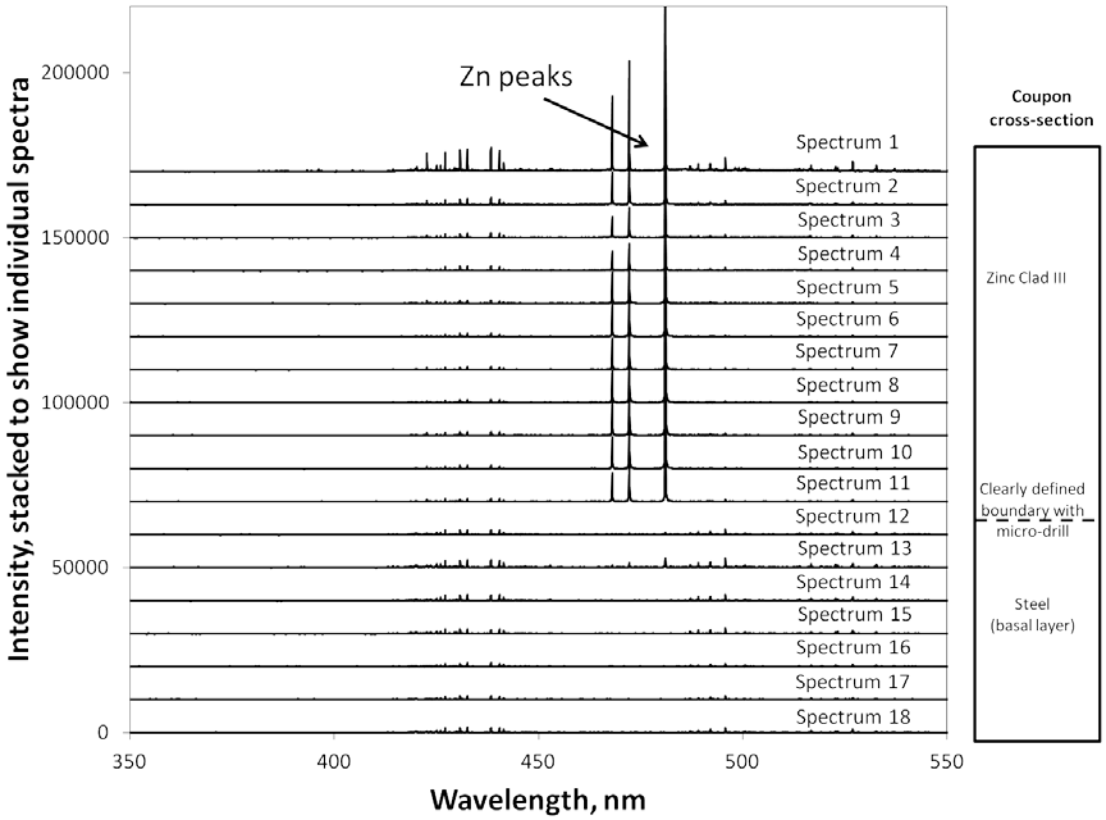

Figure 26 Spectra from Layer B produced by microdrilling.

As noted, each spectrum produced by laser drilling is contaminated by the layers above; this is reflected by the very subtle changes in the spectra (almost imperceptible when looking at spectra) with depth. The contrast between these contaminated spectra and the clear picture produced with the microdrill can be seen in PCA score plots.

Figure 27 shows a score plot for every tenth spectrum from Layer B produced by laser drilling, numbered by spectrum number. The first shot is in the upper left of the diagram, distinguished from the others by high Na from fingerprints, shown in Figure 25. All other spectra plot in a single large group, in random order. In comparison, the score plot for spectra from Layer B produced by microdrilling is presented in Figure 28. Here, the surficial (first) shot still plots by itself, but the other spectra group into two coherent groups: the Zn-rich primer, and steel. As in Figure 26, the upper Macropoxy Pre-Primer layer was not sampled because the drill penetrated the Macropoxy layer before the first laser shot.

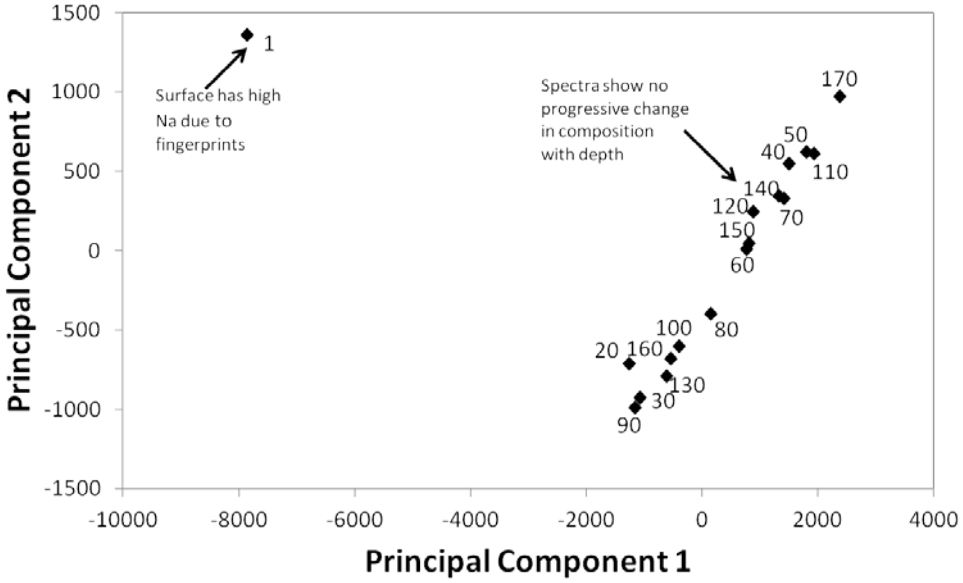

Figure 27 Principal Component Analysis score plot for spectra of Layer B produced by laser drilling.

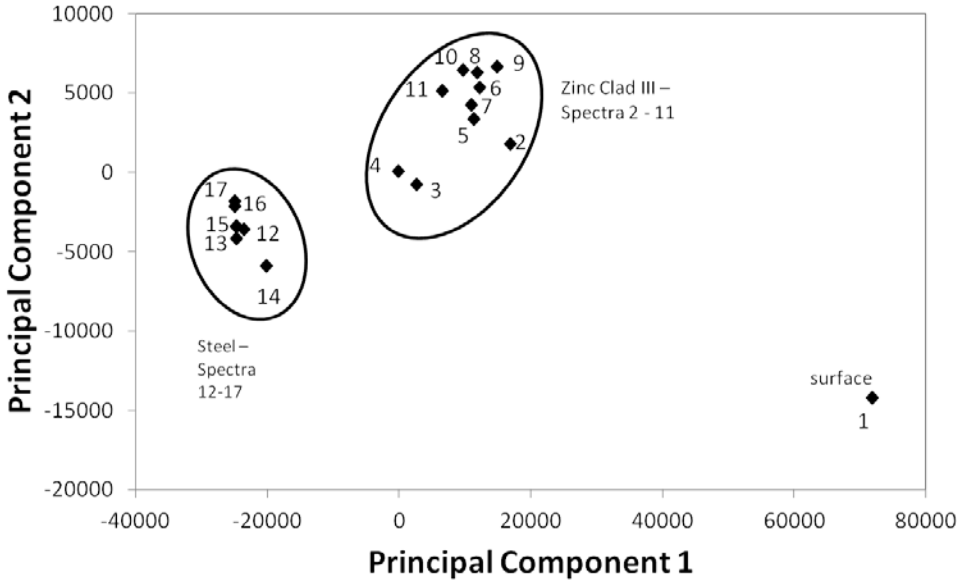

Figure 28 Principal Component Analysis score plot for spectra of Layer B produced by microdrilling.

Drilling through Layer C

Analysis of Layer C produced similar results. Figures 29 and 30 show the spectra for laser drilling and microdrilling, respectively. The spectra for laser drilling change in minor ways, but the spectra from microdrilling clearly show changes in composition with depth. There are three clear layers: Macropoxy, the Zn-rich epoxy, and steel. The PCA score plots for Layer C, shown in Figures 31 and 32, respectively, show a weak trend with depth for laser drilling, and three distinct groups for microdrilling.

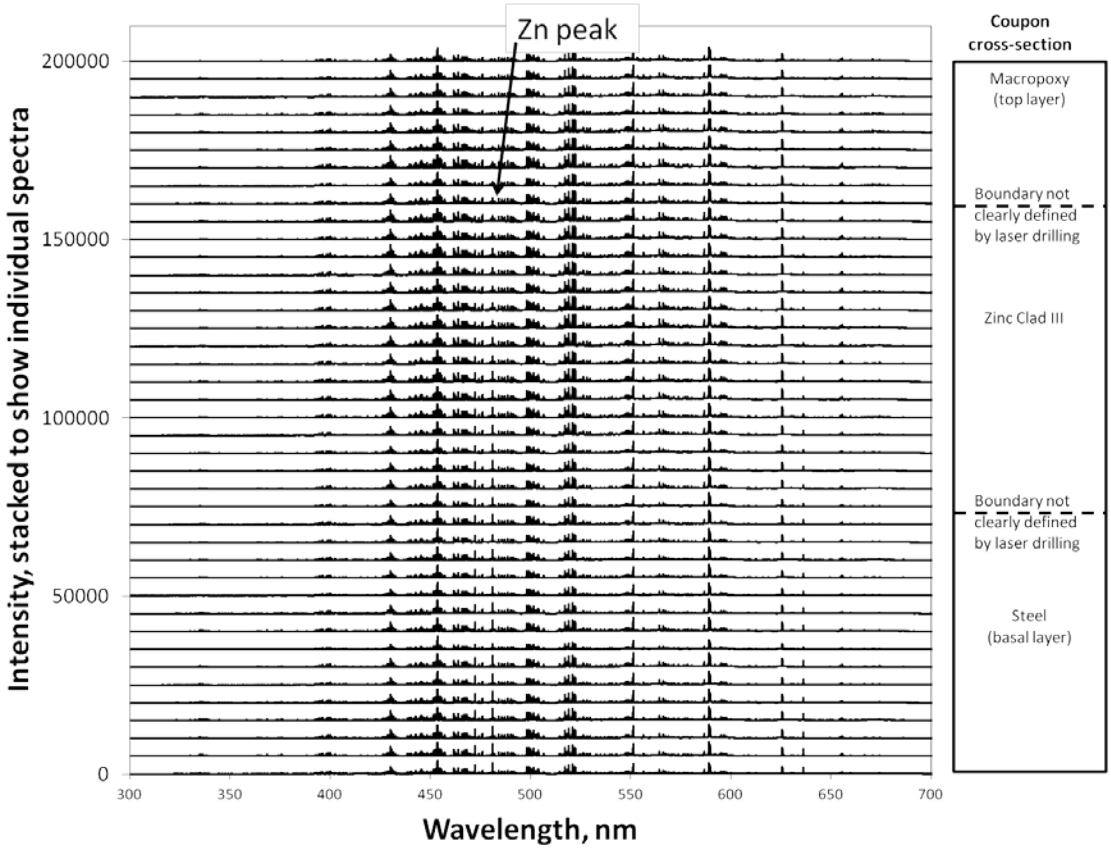

Figure 29 Spectra from Layer C produced by laser drilling.

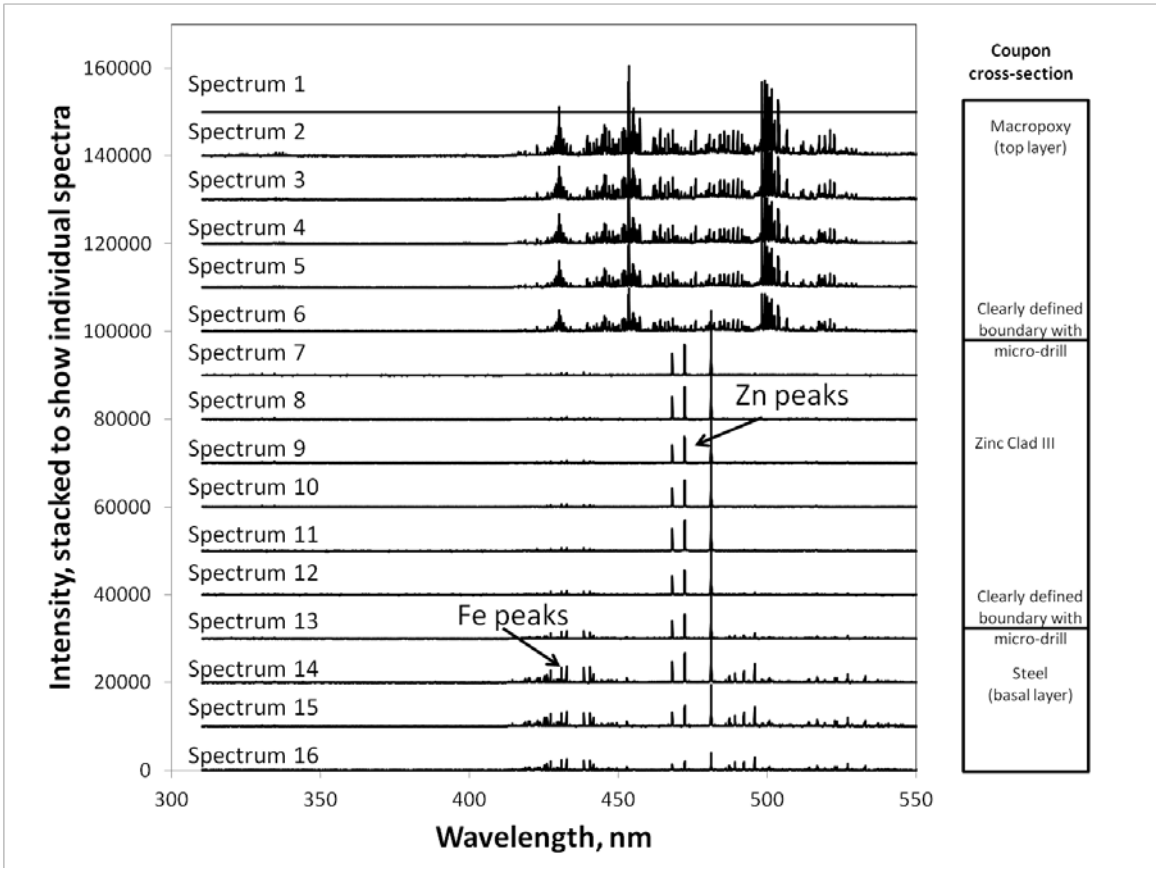

Figure 30 Spectra from Layer C produced by microdrilling.

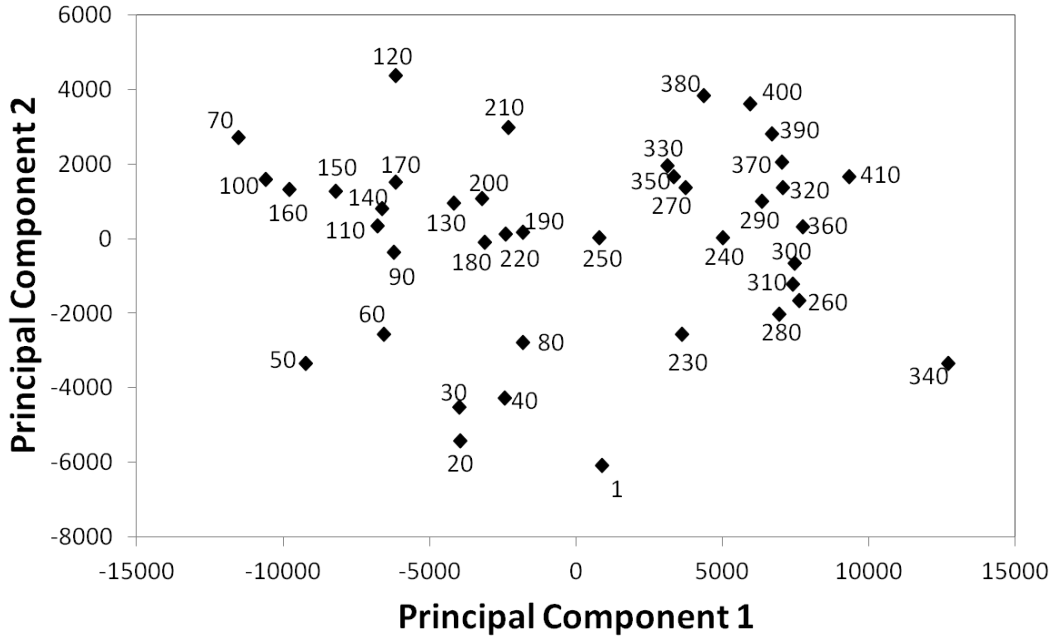

Figure 31 Principal Component Analysis score plot for spectra of Layer C produced by laser drilling.

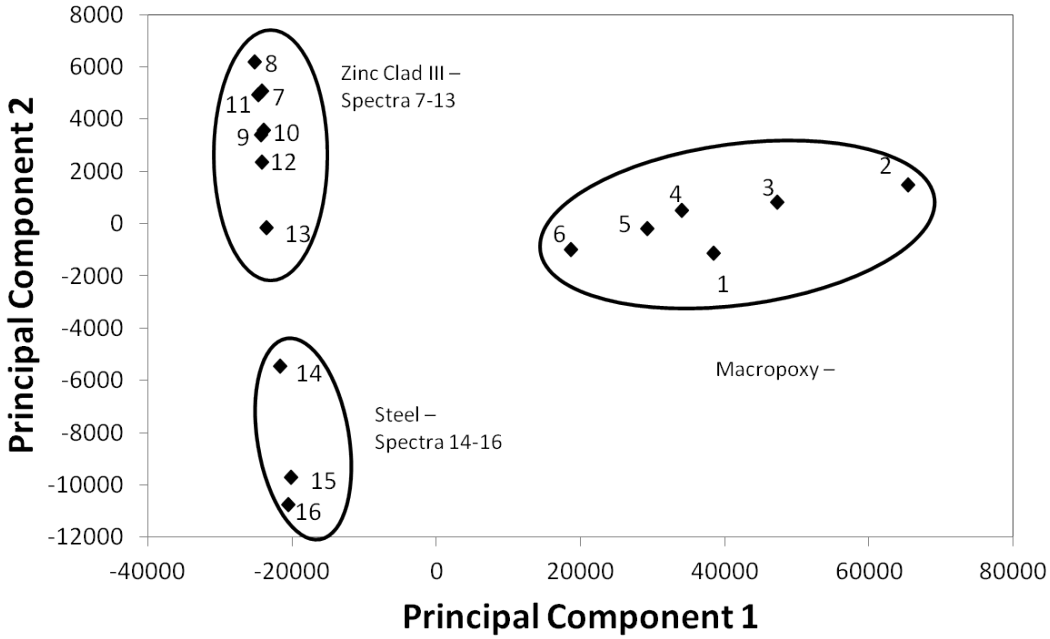

Figure 32 Principal Component Analysis score plot for spectra of Layer C produced by microdrilling.

FINDINGS AND CONCLUSIONS

Research was conducted on the feasibility of using Laser-Induced Breakdown Spectroscopy (LIBS) as a part of a system to generate a real-time bridge coating and steel corrosion inspection tool to facilitate bridge inspection operations. As part of this research an examination was made of the feasibility of

1. Heavy metal analyses in bridge coatings,
2. Titanium dioxide analysis,
3. Coating identification,
4. Corrosion indexing, and
5. Depth profiling.

Research findings were as follows:

- Heavy Metal Analysis
  Laser spectroscopy easily distinguishes between coatings with high levels of Pb, Cd, and Cr, and modern coatings with minimal levels of these elements.

- Titanium Analysis
  This pilot study demonstrates promise for quantitative analysis of TiO_2 in coatings. Concentrations measured by laser spectroscopy are proportional to those measured by ICP-MS at concentrations lower than 20%. Further work would assist in perfecting the method.

- Coating Identification Analysis
  This study attempted to classify spectra from seven types of coatings: acrylic, alkyd, epoxy, latex, urethane, varnish, and Zn-rich primers. It is possible to distinguish Zn-rich primers and alkyds from the others, but the samples of epoxy, latex, urethane, and varnish used in this study were too similar to be distinguishable using the methods employed in this investigation. Complicating factors may be the effect of Ti and elements added as coloring agents. Additional spectral analysis is required to fully address this issue.

- Corrosion Indexing Analysis
  This study demonstrates that it is possible to distinguish between corrosion Levels B, C, and D (based on visual descriptions contained in SPCC-VIS-1) with success rates around 90%. The advantage of the laser spectroscopy method over visual inspection is that one could drill through coatings to measure the corrosion spreading under the coating to detect corrosion at an early stage.

- Depth Profiling Analysis
  One of the more significant findings in this study was recognizing that laser drilling does not yield a clean spectrum of the material at the bottom of the drill hole. Spectra are contaminated by all the materials above the target surface as the laser ablates the rough edges of the hole in addition to the material at the bottom. To remedy this problem, the Research Team has developed a microdrill-laser system that alternately drills or etches out a depression on the order of 1/1000th of an inch or 25.4 microns, and then takes a laser shot of the newly exposed material. Spectra acquired with the microdrill show sharp differences as the drill penetrates new layers.

It was concluded from these findings that

- An integrated microdrill-laser system could be deployed as a powerful tool in corrosion analysis.
- Such a tool has applicability as a research tool and field inspection tool to assess the
  - presence of coatings containing high levels of heavy metals such as Pb, Cr, and Cd;
  - thickness of the coatings;
  - presence of Zn-based coatings; and the
  - type of corrosion at the site, at the surface and under the coating layers.
- The depth profiling technology featured in this research effort has the potential for use as a diagnostic tool in a variety of structures including concrete surfaces, asphalt surfaces, and steel surfaces.

PLANS FOR IMPLEMENTATION

Results of this research effort suggest that laser-scanning technology can be adopted to provide direct measurement of the type of bridge coatings, the thickness of each respective coating and the condition of the underlying steel structure (i.e., the level of corrosion).

During this effort, the Research Team developed a bench prototype system that combines a microdrill and laser operations that can achieve rapid depth profiling of a multilayer system. In addition to surface coatings, such a system can be used in many other potential applications including the examination of concrete bridge deck surfaces and subsurfaces to investigate concrete deterioration and salt penetration.

The current system prototype is presently an effective laboratory tool and can be used as such to depth profile layered paint coatings as well as other materials in the laboratory. To transition this technology to field application will require further adaptation of the current system prototype to a field system. The Research Team has initiated intellectual property protection activities (patent application) and plans to continue development and adaptation of the subject system.